ELSEVIER

Contents lists available at ScienceDirect

Fuel

journal homepage: www.elsevier.com/locate/fuel



Full Length Article

The influence on combustion and emissions of alkyl chain length in gamma and delta lactones in a heavy-duty diesel engine

Timothy Deehan*, Paul Hellier, Nicos Ladommatos

University College London's Mechanical Engineering Department, Roberts Engineering Building, University College London, Torrington Place, London WC1E 7JE, UK

ARTICLE INFO

Keywords: Compression ignition Heavy-duty engine Biofuels Lactones Combustion Emissions

ABSTRACT

Heavy-duty engines used in transport are particularly challenging to decarbonise as they cannot be easily replaced by alternative powertrains, and it remains likely that many industries will remain reliant on conventional fuels for the foreseeable future. To reduce the emissions of CO2 from heavy-duty engines, the approach of using biofuels is of interest as this would require little modification to existing vehicle fleets. Biodiesels (fatty acid methyl esters) are already widely used as a drop in biofuel for diesel, but continual growth in supply is limited by feedstock scarcity, as vegetable oils compete with the food supply. Lactones are a class of cyclic esters which can be produced from second generation biomass, a globally abundant feedstock. As esters their chemical reactivity and stability is similar to that of common biodiesels, and previous literature suggests these compounds have desirable ignition qualities and as oxygenates lower particulate emissions. In this study, the combustion and emissions characteristics of a series of isomeric gamma and delta lactones with increasing alkyl chain lengths, from C4 to C8, as single component test fuels in a heavy-duty compression ignition engine. It was found that increasing the length of the alkyl substituent chain adjacent to the ring bound oxygen within the lactones reduced the duration of ignition delay, resulting in a smaller premixed burn fraction during combustion and decreasing emissions of nitrogen oxides, unburnt hydrocarbons and carbon monoxide. For the majority of the lactones an equivalent isomer was also tested, allowing for comparisons on between equivalent carbon count or substituent alkyl chain length. Gamma lactones compared to delta lactones of the same carbon number exhibited a shorter duration of ignition delay and apparent peak heat release rate. When comparing lactones of different ring size with the same length of the substituent alkyl chain, the delta lactones initially exhibited a shorter duration of ignition delay, longer duration of combustion and lower unburnt hydrocarbons and carbon monoxide emissions.

1. Introduction

The concentration of CO_2 in Earth's atmosphere has increased drastically since the start of the industrial revolution and widespread consumption of fossil fuels commenced. As CO_2 absorbs radiation from the earth in the infrared spectrum, it is classed as a greenhouse gas, and a high concentration in the atmosphere contributes to global temperature rise. [1] There is extensive evidence supporting this rise and the associated implications, such as rising sea levels, glacial melt and disruption of oceanic currents, which have driven forward research into the reduction of anthropogenic CO_2 production. [2,3].

In 2019 the European Union attributed 25 % of its total $\rm CO_2$ emissions to the transport industry, and set goals of reducing emissions by 55 % by 2030. [4] The most recent agreement on amendments to the

Renewable Energy Directive calls for fuel consumption in the transport industry to meet either a 14.9 % greenhouse gas emission reduction or for 29 % of the final energy consumption to be renewable. [5].

Heavy-goods vehicles represent a challenging sector for this uptake in renewable energy. In order to reduce the emissions of CO_2 contributed from goods vehicles, the approach of using biofuels is of increasing interest as this would require little modification to existing vehicle fleets. Whilst not all biofuels emit the same amount of CO_2 during combustion, biofuels exist in a closed carbon cycle. The CO_2 emissions resultant from biofuel production and use are ideally equal to or less then the carbon from the atmosphere by the growth of the biological source of the fuel.

There is often debate on whether crops high in sugars and starches should be grown for use as biofuels, as this crop mass competes with food production for society. This leads current biofuel efforts to focus on using plant biomass sources which do not compete with food

E-mail address: timothy.deehan.17@ucl.ac.uk (T. Deehan).

^{*} Corresponding author.

Nomenclature			Gamma decalactone	
		γHpl	Gamma heptalactone	
APHRR	Apparent peak heat release rate	γHxl	Gamma hexalactone	
BTDC	Before top dead centre	γNl	Gamma nonalactone	
CAD	Crank angle degree	γOl	Gamma octalactone	
CO	Carbon monoxide	γUl	Gamma undecalactone	
CO_2	Carbon dioxide	γVl	Gamma valerolactone	
C-SOC	Constant start of combustion	GHG	Greenhouse gas	
D8k	Volvo D8k engine	ID	Ignition delay	
DAQ	Data acquisition	IMEP	Indicated mean effective pressure	
δDdl	Delta dodecalactone	NO_x	Nitrogen oxides	
δDl	Delta decalactone	O_2	Oxygen	
δNl	Delta nonalactone	PAH	Polyaromatic hydrocarbons	
δUl	Delta undecalactone	PRV	Pressure relief valve	
Dyno	Dynamometer	Ref. D	Reference diesel	
ECU	Engine control unit	RPM	Revolutions per minute	
ETU	Engine timing unit	SOC	Start of combustion	
γDdl	Gamma dodecalactone	THC	Unburnt hydrocarbons	

availability.

A group of compounds which is widely abundant in nature are lactones, defined as any class of cyclic organic compound which contain an ester group, found widely in natural sources such as fruit, wood and foodstuffs as key building blocks for hormones, neurotransmitters and enzymes. [6,7] Cyclic esters remain a broad category, and many methods of producing lactones have been identified, especially in therapeutic drug discovery. [8] A review of industrial processes for producing natural flavour compounds by Schrader et al. stated that optimisation of γ -decalactone production resulted in average prices falling from \$10,000/kg in the 1980 s to an average of \$300/kg by the time of publication in 2003. [9] Producing lactones for various purposes has since grown in interest; Silva Souza et al. found that there has been close to three research publications and 15 patents filed each year since 2003 related to the biotechnological synthesis of γ -dodecalactone. [10] In their review of lactone production from an industrial perspective, Sved et al. state that the most commercially import lactones are γ - and δ-dodecalactone, predominately produced by a chemical synthetic route using castor oil as a starting material. [11] Syed et al. state that prices for synthetically produced volumes of these lactones were close to \$150/kg in 2023, but that the global market remained limited by castor oil availability. [11].

Lactones have remained an interesting topic for future fuels research, for their abundant bioavailability, for example a patent filed in 2013 included some gamma-lactones as a few of many popular perfume ingredients suggested as potential gasoline and diesel blending components. [12,13].

The lactone structure is commonly found in many natural sources, resulting in an abundant range of lactones, which vary both in ring side or contain additional side groups. [14,15,8] However, despite the wide dearth of lactones available, the majority of biofuels or combustion studies to date considering lactones have focused solely on gamma-valerolactone (γ VI).

 γVl has remained a popular subject of research in spark ignition (SI) engines as a blended fuel, for the ease with which it can be produced from biomass, its anti-knock properties and comparable physical properties to ethanol. Structural isomers of γVl such as angelica lactones and butyrolactones have a plethora of known synthetic routes from itaconic acid and levullinic acid starting points, two compounds which are easily isolatable from most lignocellulosic biomass. [17].

 $\gamma Vl,$ as noted, is a theoretically ideal candidate for spark ignition engines, and the fuel has shown some significant results for SI engines, but wider adoption of the fuel is unlikely, owing to the wider use of ethanol. [16,18] Additionally, SI engines are themselves an ideal candidate for electrification. [19] Future fuels research should instead focus on compression ignition (CI) engines, as these are used in markets which present much higher barriers to electrification, especially in offroad sectors where charging infrastructure is impractical. [19,20].

Research into the fuel performance of lactones with long alkyl chains and high molecular weight which will exhibit preferable characteristics for CI engines have been discussed in concept, yet these larger lactones have previously not received attention as single component biofuels. Larger lactones can be isolated from biomass sources and there is continual research into one-pot synthetic routes. Publications focusing on biofuel production from these lactones has instead focused on catalytic conversion of such compounds to saturated alkanes prior to testing. [13,21,22].

Early tests of lactones in CI engines were undertaken by Bereczky et al., who investigated the ability of γVI to reduce CI engine particulate emissions. γVI was tested in a 10:3:1 mixture of fossil diesel, biodiesel and γVI respectively. [23] Bereczky tested the blend against pure fossil diesel and a 10:3 diesel & biodiesel mixture, finding that the γVI mixture had substantially lower THC emissions at different engine speeds. When lower loads at a constant speed of 2,500 rpm were tested, the γVI mixture did not significantly lower THC emissions compared to the biodiesel only mixture. The γVI mixture did emit higher CO emissions at all the engine speeds tested up to 2,500 rpm, but was indistinguishable from the other mixtures at 3,000 rpm. NOx emissions were indistinguishable from each fuel at the same loads. Overall, Bereczky et al. concluded that compared to fossil diesel the exhaust smoke concertation was reduced with the biodiesel blend and further reduced with the γVI blend.

Frost et al. investigated a series of lactones which contained higher carbon numbers than γVl , or were substituted with long hydrocarbon chains, and for the first time demonstrated the combustive performance of C10 and C12 lactones in a high-speed automotive diesel engine (2 L displacement with an 18.3:1 compression ratio). [24] The tests were performed on lactones blended with butanol and diesel, in a ratio of 1:2:3 of butanol, lactone and diesel respectively. When comparing lactones with the same carbon number, but a decreasing chain size (thereby the lactone ring expanding) Frost et al. found a slight decrease in ignition delay, similar CO emissions, and no observable trends in particulate mass or particulate number. [24].

When comparing similar lactone ring sizes with differing substituent hydrocarbon chain lengths, the results of Frost et al. clearly demonstrated a strong relationship between a long side-chain length and a shorter duration of ignition delay. This result can be expected, as increasing the number of freely available –CH2 groups increases cetane

number, as is evident in aliphatic hydrocarbon cetane numbers. [25] A more intriguing result was that of the gamma-dodecalactone (γ Ddl) blend exhibiting a shorter duration of ignition delay than the reference fossil diesel, even though the reference blend of only diesel and butanol exhibited a significantly longer ignition delay period – indicating that γ Ddl would possibly exhibit a shorter duration without the other blend components.

This is the first work to systematically test the combustion of single component gamma and delta lactones as potential renewable fuels, and link changes in combustion characteristics to molecular structure, which is of itself novel. The gamma and delta lactone rings are significantly more stable than lactones with other ring sizes and both can be isolated or produced from biomass sources, [26] and were chosen as single component fuels to provide insight into lactone ring size and alkyl chain length on combustion in a heavy-duty compression ignition engine.

2. Heavy-duty compression ignition engine test facility

All of the combustion experiments presented were performed in a heavy-duty compression ignition engine which was appropriately modified for supplying test fuels to one of the six engine cylinders while the remaining were supplied with fossil diesel to ensure smooth engine operation. The operation of the facility was unchanged from that reported previously in Deehan et al. (2024), but is repeated here for clarity. [27] The volume of diesel supplied to the back five cylinders (two to six) was a much smaller volume than the amount of test fuel supplied to cylinder one, thereby keeping the total engine output torque below the maximum limit for the water-cooled Schenk Eddy Current Dynamometer W130 which controlled engine speed.

In-cylinder pressure data was monitored with a Kistler type 6052C pressure transducer installed adjacent to the cylinder one exhaust valves. Injection timing, injection duration and cylinder firing order was controlled by an AVL engine timing unit, timed according to a digital signal from a Turck proximity sensor on the camshaft and a Baumer

EIL580-T Optopulse crankshaft encoder with a 0.1CAD resolution. Experimental data from the timing unit and pressure transducer was recorded in a custom LabView environment. Pressure data for cylinder one was averaged over 100 continuous combustion cycles during each experiment, which was used to calculate the global net apparent heat release rate (AHRR) and in-cylinder temperatures exhibited during combustion, using standard heat capacities and values of gamma for exhaust gasses, as presented in Heywood (2018). [28].

Fig. 2.1 depicts the testing facility, and the divided common rail system and low-volume fuel system used to supply the single component test fuels to the D8k. A separate low-volume test fuel system was used in order to avoid damage to the engine high-pressure fuel pump when using low lubricity and corrosive test fuels, and also so as to minimise the required volume of costly test fuels. The operation of the low-volume test fuel system remains unchanged from that previously reported in detail by Hellier et al. (2011) [29] and Schönborn et al. (2007) [30] Gaseous emissions were measured with a Horiba MEXA 9100 HEGR, incorporating individual instruments to analyse concentrations of each of the CO, CO₂, O₂, NO and NO_x. THC was measured in a Horiba FIA Ov-04 flame ionisation detector.

2.1. Test fuels

Twelve lactones were tested as pure components to investigate the effect of increasing the substituent alkyl chain length for two different ring sizes on compression ignition combustion and emissions. Table 2.2 provides an overview of these single component fuels and their chemical structure. Three further lactones, not shown in Table 2.2, Delta octalactone and either gamma or delta tridecalactone, were considered for the experiments but were not commercially available at reasonable cost, nor were they known to be widely bio-available.

Two sets of similar molecules were used, eight gamma lactones with an alkyl chain length increasing from one to eight carbons, and four delta lactones with a chain length increasing from four to seven carbons.

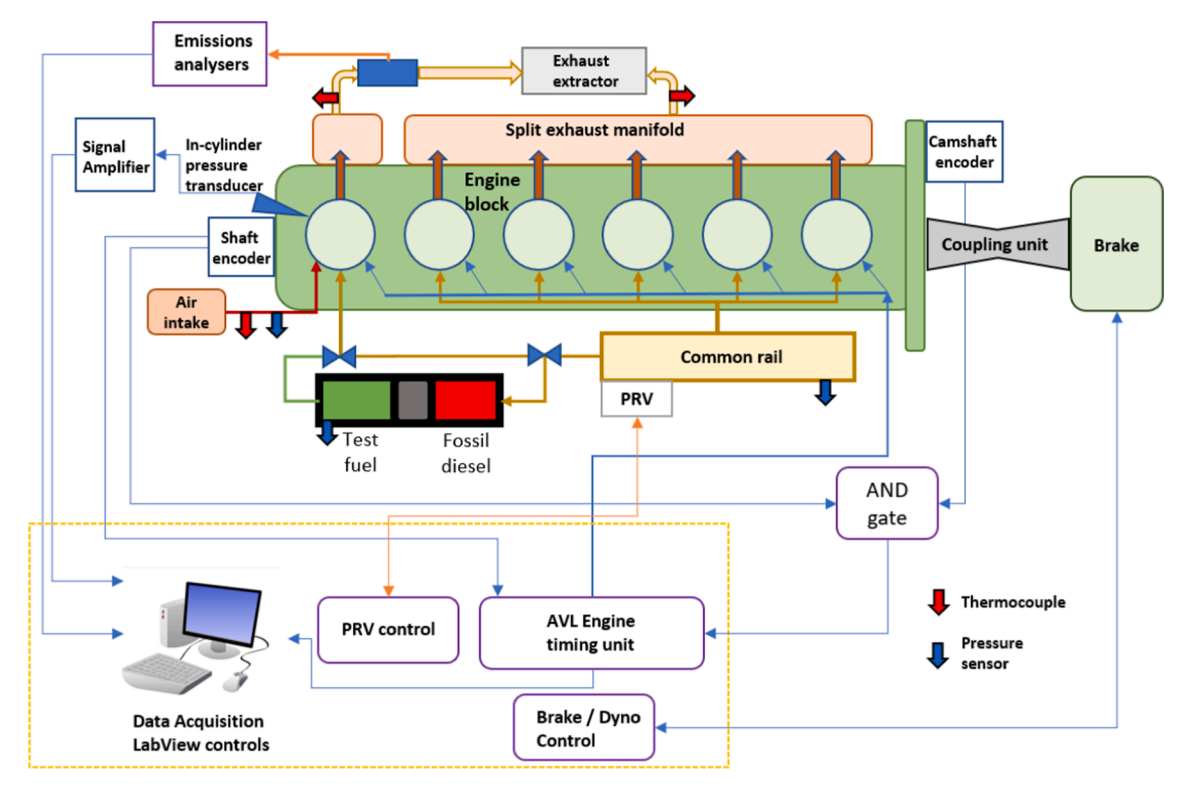


Fig. 2.1. Overview of the testing facility, showing signal flow between the control components. All thermocouples and pressure sensors signal lines have been omitted for clarity, each of these sends a unidirectional signal to the LabView controls. Shown is the high-volume fuel system which delivered test fuel directly to cylinder 1 only. Abbreviation: pressure relief valve (PRV).

Table 2.1 Engine specification.

Engine model	Volvo D8k 320	
No. of cylinders	6	
Displacement	7.7 dm ³	
Compression ratio	17.5:1	
Firing Order	1, 4, 2, 6, 3, 5	
(Where cylinder 1 is that furthest from the flywheel)		
Engine Dimensions h*w*l (mm)	1004.06 * 830 * 1252.17	
Combustion chamber geometry (mm)		
Piston diameter	108.195 ± 0.012	
Con Rod length	213.5	
Cylinder bore	110	
Crank radius	67.5	
Clearance volume (mm ³)	775.7	
Piston bowl geometry	Re-entrant design	
Injection pressure	700 ± 5 bar	
Shaft encoder	0.1 CAD resolution	
Engine speed	$820\pm20~\text{RPM}$	

Table 2.2Overview of the single component lactone test fuels alongside an abbreviation for each fuel and a skeletal depiction of their molecular structure.

Fuel	Alkyl chain	Chemical structure
(Nomenclature)	n =	
Gamma-Valerolactone (γVI)	N/A	0
Gamma-Hexalactone (γHxl)	N/A	0
Gamma-Heptalactone (γHpl)	1	0 0
Gamma-Octalactone (γOl)	2	7 T M
Gamma-Nonalactone (γNl)	3	\/ \ \ \ / n
Gamma-Decalactone (γDl)	4	
Gamma-Undecalactone (γUl)	5	
Gamma-Dodecalactone (γDdl)	6	
Delta-Nonalactone (δNl)	2	
Delta-Decalactone (δDl)	3	
Delta-Undecalactone (δUl)	4	
Delta-Dodecalactone (δDdl)	5	n

These 12 single component fuel tests allowed observation of the resulting effects from increasing the alkyl chain length on these lactones. The different ring size and overlap in alkyl chain length between the two different lactone series allowed comparison between the gamma and delta lactones with the same chemical formula or equivalent chain length. Gamma and delta nonalactone are both a chemical formula of $C_9H_{16}O_2$, but different alkyl chain lengths, so differences in fuel performance arising from chain length and ring size may be inferred. Likewise, gamma nonalactone and delta decalactone have a substituent alkyl chain containing five carbons so differences in fuel performance from the lactone ring size may be observed.

Fig. 2.2 shows an example of four lactones which provide a useful introduction to some of the structural differences which will be referenced frequently in this work. The two important metrics of comparison

between the lactone single component fuels presented here are the lactone ring isomer and the substituent alkyl chain length.

Arrows 1 & 2 represent the structural isomerism between gamma and delta lactones with the same chemical formula and carbon count. It is important to note that by definition, the delta lactone alkyl chain will always be one –CH $_2$ group shorter than the gamma lactone. Arrows 3 & 4 represent the addition of a –CH $_2$ group in the substituent alkyl chain, increasing the total carbon count and alkyl chain length. Arrow 5 represents a gamma and delta lactone which both have the same alkyl chain length. These two are not isomers, by definition delta lactone will always have a higher carbon count.

Three comparisons are available between any two lactones:

- 1. Constant ring size with a varying chain length
- 2. Constant alkyl chain length with a varying ring size
- 3. Constant carbon count, with a varying chain length and ring size.

3. Experimental procedure

Table 3.1 shows results of the viscosity and calorific value measurements of the 12 lactones. Together with values of boiling point and density shown in the table, they are key properties for interpreting the combustion results for the lactones.

Each of the single component lactone fuels, and reference fossil diesel, were tested in the Volvo D8k engine under identical conditions of constant speed of 820 RPM, constant injection pressure of 700 bar and constant injection timing of 5.3CAD before TDC (BTDC). Of the lactones shown in Table 2.2, an attempt was made to combust gamma valerolactone, hexalactone and heptalactone as single component fuels at the same experimental conditions, but they either did not ignite or exhibited highly unstable combustion late into the expansion stroke. Table 3.2. summarises the measured key combustion parameters from the combustion experiments. The engine conditions, that of a constant injection pressure and constant engine speed, were chosen as a somewhat representable environment for studying the initial combustion characteristics of the fuels and to avoid unwanted heat release due to unknown combustion phasing, while also allowing collection of combustion data with the limited quantity of fuel available. These conditions allow the study to focus on ignition quality and overall combustion characteristics, and we note that setting the operation to constant IMEP would more closely align with real operating conditions.

A subset of four of the lactone fuels, having the lowest and highest carbon count from both series were additionally tested at constant start of combustion (SOC, defined as the minimum value of cumulative heat release after start of injection and before the time of peak heat release rate) which was maintained approximately at TDC. This necessitated a different setting of start of injection for each lactone fuel, depending on their ignition delay. Table 3.3. shows the injection and ignition timings for these constant start of combustion tests, and the measured key combustion parameters.

4. Results

4.1. In-cylinder pressure and heat release rates at constant injection timing

Fig. 4.1 shows the in-cylinder pressures and apparent heat release rates of gamma octalactone (γ Ol), nonalactone (γ Nl), decalactone (γ Dl), undecalactone (γ Ul), dodecalactone (γ Ddl) and reference fossil diesel. Immediately apparent is the significantly longer duration of ignition delay (ID, defined as the period between the start of fuel injection and the start of combustion) exhibited by γ Ol relative to the remaining lactone fuels. It can be seen that γ Ol underwent two-stage ignition, where the apparent heat release rate (AHRR) sees a positive increase at 363 CAD followed by a second distinct positive increase in AHRR at 367 CAD. As with γ Ol but not as obvious, γ Nl and γ Dl also appear to exhibit

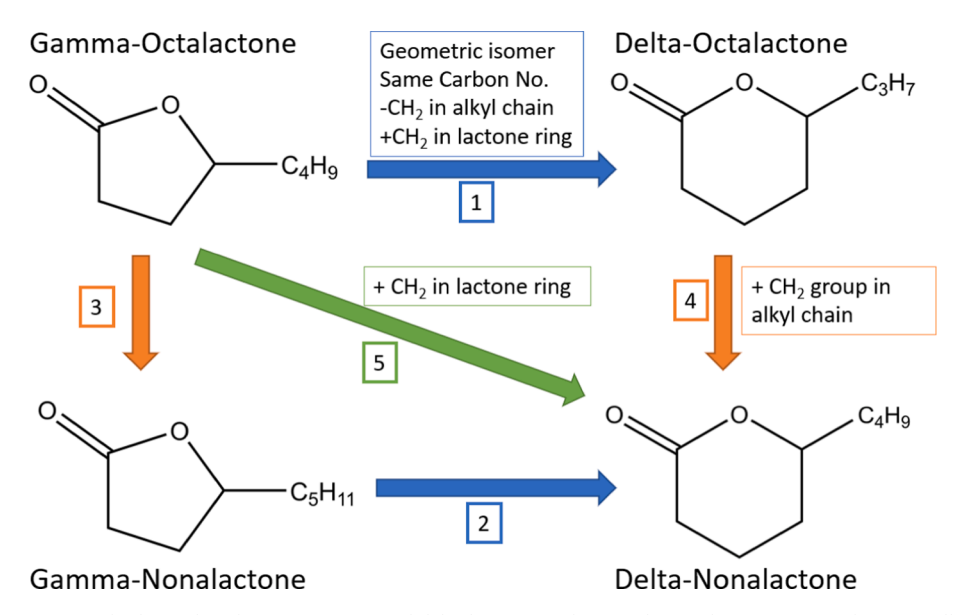


Fig. 2.2. The interconnected relationships between gamma and delta lactones with equivalent carbon counts or substituent alkyl chain lengths.

Table 3.1
Physical and chemical properties of the lactones and the reference diesel. Each lactone's purity was > 97 %, the boiling point and density data provided by the supplier, Merck. Viscosity measured using a Brookfield III-Ultra rheometer. Gross calorific value measured using an IKA C1 bomb calorimeter. *c technical data for the reference diesel provided by Haltermann Carless.

Fuel (Nomenclature)	Boiling point (°C)	Density at 25 °C (g/cm ³)	Viscosity at 50 °C (Cp)	Gross calorific value (J/g)	Derived cetane number
γ-Valerolactone (γVl)	207[31]	1.05	1.48	$26,257.00 \pm 91.84$	$< 10^{32}$
γ-Hexalactone (γHxl)	215 [32]- 219[33]	1.023	1.77	$28,\!332.97 \\ \pm 203.26$	N/A
γ-Heptalactone (γHpl)	230.2 [15]	0.999	1.86	$30,769.00 \pm 45.59$	N/A
γ-Octalactone (γOl)	248.4 [15]	0.981	2.34	$31,970.33 \pm 207.27$	N/A
γ -Nonalactone (γ Nl)	265.5 [15]	0.976	2.77	$33,234.00 \\ \pm 111.15$	N/A
γ-Decalactone (γDl)	281.7 [15]	0.952	3.18	$34,430.00 \\ \pm 112.54$	N/A
γ-Undecalactone (γUl)	290.0 [34]	0.949	3.85	$35,657.88 \pm 140.55$	52.6[25]
γ -Dodecalactone (γ Ddl)	311.5 [35]	0.936	4.48	$35,963.52 \pm 40.21$	N/A
δ-Nonalactone ($δ$ Nl)	267.0 [15]	0.994	3.39	33,496.59 ± 60.64	N/A
δ-Decalactone ($δ$ Dl)	283.2 [15]	0.954	3.54	$34,756.67 \pm 29.53$	N/A
δ-Undecalactone ($δ$ Ul)	297.0 [34]	0.969	4.29	$35,610 \pm 117.36$	48.6[25]
δ-Dodecalactone ($δ$ Ddl)	312.7 [36]	0.942	5.01	$36,404.00 \\ \pm 84.76$	N/A
Reference Diesel (Ref. D)	189.9 – 355.5°	0.832 ^c	2.245	45,800 ^c	52.2 ^c

two-stage ignition (Fig. 4.1b), suggesting that the remaining gamma lactones may also potentially undergo two stages of ignition delay, but that this is possibly masked by the short overall ignition delay of the larger lactones. For γ Dl, γ Ul, γ Ddl and the reference diesel it can be seen that once the gradient for the heat release turns positive, it continues to increase until the apparent peak heat release rate (APHRR) is reached, but for γ Ol and γ Nl the initial positive heat release is followed by a plateau or decrease in AHRR before a second positive change in AHRR

occurs. Two-stage ignition is commonly observed in tests with two separate fuels blended, such as n-heptane and toluene, and is assumed to be resultant from low temperature reactions prior to autoignition not generating significant heat to sustain the combustion process until a higher pressure and temperature are also reached. [37,38].

It is also apparent from Fig. 4.1.a that γDdl and γUl exhibit very similar in-cylinder pressures during combustion. Additionally, the premixed burn and diffusion-controlled combustion periods exhibited by γDdl and γUl closely resemble that of the reference fossil diesel, whilst γDl , γNl and γOl each display a significantly larger premixed burn fraction than the fossil reference diesel (Fig. 4.1.b) due to their longer ignition delays providing longer period for fuel premixing and, possibly, due to their somewhat lower boiling points.

Considering the molecular structures of the gamma lactones, it is visible from Fig. 4.1 that each addition of a $-CH_2$ group to the substituent alkyl chain from γOl to γDdl shortens the duration of ignition delay, leading to a smaller premixed burn fraction combustion period.

Fig. 4.2 shows the in-cylinder pressures and apparent heat release rates of delta nonalactone (δ Nl), decalactone (δ Dl), undecalactone (δ Ul), dodecalactone (δ Ddl) and reference fossil diesel. Apparent is the increase in duration of ignition delay and associated size of the premixed fraction of combustion as the substituent alkyl chain length decreases from δ Ddl to δ Nl, similar to that previously shown for the gamma lactones (Fig. 4.1).

However, unlike the gamma lactones, no two-stage ignition is visible amongst any of the delta lactone test fuels. Furthermore, the premixed burn and diffusion-controlled periods of combustion exhibited by δDdl and δUl show a more distinct difference relative to the fossil diesel than the gamma lactones of equivalent carbon number (γUl and γDdl respectively).

Fig. 4.3 Shows the net apparent heat release rate of both the gamma and delta nonalactones, decalactones, undecalatones, dodecalactones and the reference fossil diesel tested at a constant injection timing. The trend apparent is that for each pair of lactones with an equivalent carbon number (e.g., gamma and delta dodecalactone), the gamma lactone exhibits a shorter period of ignition delay and consequently a smaller premixed burned fuel fraction. As shown in Table 3.1, γ Nl and δ Nl have the same C:H:O ratio, as does γ Dl and δ Dl and so on, therefore differences in fuel behaviour must arise from differences in chemical structure.

The difference in lactone ring size between the equivalent carbon number gamma and delta lactone is associated with a difference in the length of the alkyl chain substituent. As shown in Table 2.2, for example,

Table 3.2
Experimental test conditions and key experimental results for the single component fuel tests in the D8k engine at constant injection timing of 5.3 CAD BTDC, constant injection duration of 6.5 CAD and brake controlling a constant engine speed.

Fuel (Acronym)	IMEP	Ignition delay	Duration of combustion	APHRR	Timing of APHRR	Maximum global calculated in-cylinder temperatures
	(bar)	(CAD)	(CAD)	(J/	(CAD)	(K)
				CAD)		
γ-Valerolactone (γVl)	Did not combust	-	_	-	_	_
	(DNC)					
γ-Hexalactone (γHxl)	DNC	_	_	_	_	_
γ-Heptalactone (γHpl)	DNC	_	_	_	_	_
γ-Octalactone (γOl)	4.93	9.2	17.2	543.50	369.9	1760.8
γ-Nonalactone (γNl)	5.16	6.7	26.5	624.27	364.1	1728.6
γ-Decalactone (γDl)	5.34	6.2	26.6	501.30	363.2	1736.6
γ-Undecalactone (γUl)	5.64	5.4	27.8	310.58	361.9	1763.1
γ-Dodecalactone (γDdl)	5.71	5.0	28.5	259.89	361.5	1768.5
δ-Nonalactone (δNl)	5.34	7.7	25.3	750.16	365.4	1786.0
δ-Decalactone (δDl)	5.51	6.5	26.90	539.38	363.5	1744.6
δ-Undecalactone (δUl)	5.60	6.0	27.50	397.01	362.6	1742.3
δ-Dodecalactone (δDdl)	5.63	5.5	28.30	314.56	362.1	1741.9
Reference Diesel	7.18 ± 0.09	5.2 ± 0.09	32.78	328.42	361.62	1902.1
(Ref. D)						

Table 3.3

Experimental test conditions and key experimental results for the single component fuel tests in the D8k engine at constant injection duration of 6.5 CAD and a variable injection timing chosen to ensure combustion of each lactone occurs at TDC. Gamma-octalactone has two entries as advanced the injection timing led to gamma-octalactone exhibiting two-stage ignition. Two timings were chosen, so that either the first stage or second stage of ignition occurred at TDC.

Fuel	Injection timing (CAD BTDC)	IMEP	Ignition delay (CAD)	Duration of combustion (CAD)	APHRR	Timing of APHRR (CAD)	Maximum global calculated in-cylinder temperatures (K)
		(Bar)			(J/CAD)		
δNl	7.8	5.06	7.5	23	739.54	367.8	1782.5
δDdl	5.5	5.60	5.5	28.2	308.03	374.5	1748.6
γOl	9.1	5.04	9.1	16.9	760.56	367.8	1849.5
	11.7	4.78	9.1	15.9	752.49	364.8	1871.0
γDl	5.2	5.50	5.2	28.4	262.57	374.7	1738.2
Ref. D	5.3	$\textbf{7.18} \pm \textbf{0.09}$	5.2 ± 0.09	32.78	328.42	361.62	1902.1

the alkyl chain in γNl contains 3 –CH₂ groups, whilst δNl contains 2 of these groups. It has previously been shown that increasing the available number of alkyl chain –CH₂ groups leads to a reduction in duration of ignition delay as there are more sites in each single fuel molecule for combustion to initiate. [29] Alkyl free chains have higher mobility than organic rings such as lactones, so it can be assumed that the intermediate cyclic species formed during the low temperature pre-ignition kinetic reactions can more readily propagate combustion on the alkyl chain than the saturated ring. [39] It is therefore to be expected that the gamma lactones will experience easier autoignition than the delta lactones of the same carbon count, where carbon atoms are conceptually moved from the ring to the alkyl chain.

However, of note in Fig. 4.3 is the heat release exhibited by $\gamma Ul,$ which as expected exhibits a shorter duration of ignition delay than $\delta Ul,$ but unexpectantly also a slightly shorter delay than δDdl (Table 0.3). δDdl and γUl both have an alkyl chain containing 7 carbons, but as shown in Table 3.1 δDdl has a higher total carbon count and higher calorific value.

4.2. In-cylinder pressure and heat release rates at constant start of combustion

Fig. 4.4 shows the in-cylinder pressure and apparent net heat release rates of delta nonalactone (δ NI), delta decalactone (δ DI), gamma octalactone (γ OI), gamma dodecalactone (γ DdI) and reference fossil diesel at a constant start of combustion (SOC) timing at TDC (360 CAD), using the injection timings outlined in Table 3.3. For each fuel the injection timing was varied so that the start of combustion always occurred at TDC. Owing to the significant two-stage ignition observed from γ OI, which results in the bulk of the heat release occurring into the expansion stroke, γ OI was tested twice; once so that the 1st stage ignition event

occurred at TDC, and secondly such that the 2nd stage ignition and therefore main heat release event occurring close to TDC. Advancing the fuel injection timings such that all fuels ignite at the same CAD allows for discussion on how this affects fuel emissions. All the test fuels ignited within 0.3 CAD of TDC, except for γ Ol with second stage SOC at 357.4. Predicting the change in two-stage ignition exhibited by γ Ol when injection timings was adjusted to achieve SOC at TDC proved difficult and led to this disparity in SOC timing from TDC.

The most apparent feature of Fig. 4.4 is the significantly larger premixed burn fraction of combustion exhibited by γ Ol and δ Nl compared to the reference diesel, γ Ddl and δ Ddl. This is due to their considerably longer ignition delay periods. Adjustment of injection timing does not appear to have affected the two-stage ignition exhibited by γ Ol, however bringing forward the injection timing does increase the observed AHRR compared to the constant injection timing condition (Fig. 4.1).

At constant SOC, the observed heat release rates exhibited by γDdl and δDdl appear very similar to that of the reference diesel.

4.3. Combustion characteristics

Fig. 4.5 shows the impact of overall carbon number and alkyl chain length on ignition delay in substituted gamma and delta lactones at constant injection timing. In Fig. 4.5, and all subsequent figures, the error bars show the standard deviation about the mean of repeat tests of the reference diesel performed alongside to the lactone fuel tests. The error bars present on the diesel results is calculated from the reference diesel at the start and end of six days of testing, and therefore 12 repeats of a representable 100 continuous combustion cycles. The ignition delay of gamma octalactone (γ Ol), delta nonalactone (δ Nl) and gamma nonalactone (γ Nl) showed a slight instance of variability within the 100 consecutive combustion cycles recorded and the coefficient of variance

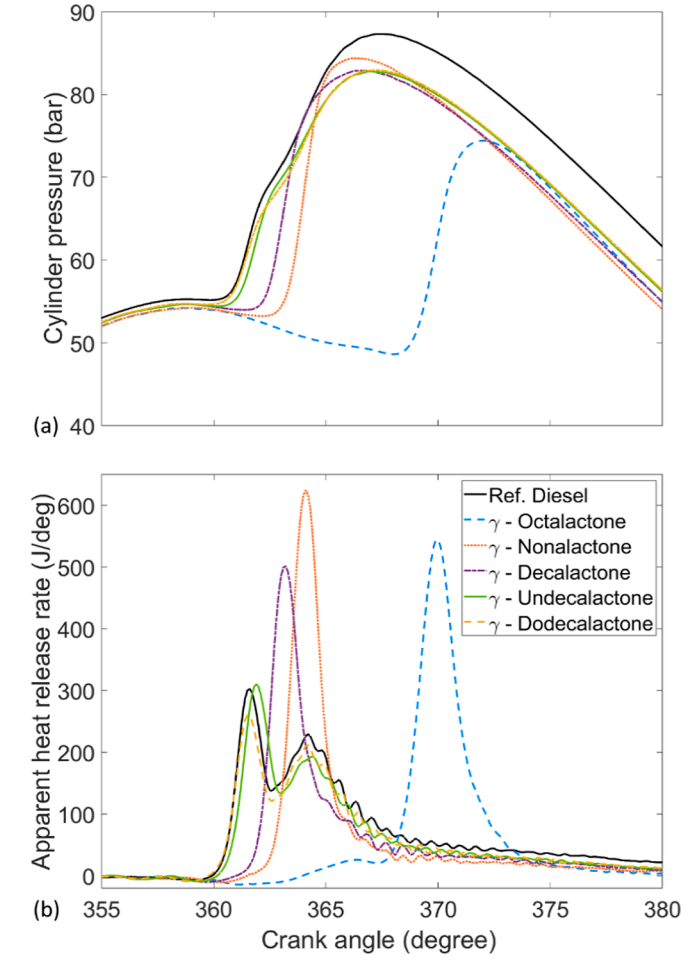


Fig. 4.1. (a) In-cylinder pressures and (b) apparent heat release rates of the single component gamma lactone test fuels and reference fossil diesel.

was found to be 0.1239, 0.1097, and 3.946 respectively. For the remaining test fuels and reference diesel the coefficient of variance was 0.

Apparent in Fig. 4.5a is a general trend of decreasing ignition delay with increasing size for both lactones. There is a consistent offset in corresponding delay values, where the gamma lactones exhibit shorter ignition delays than the delta lactones, which is in agreement with the findings of Frost et al. [24] As shown in Table 2.2, the difference in ring size between the equivalent gamma and delta lactones means the gamma isomer will have a longer substituted alkyl chain length than the delta isomer at equivalent carbon counts. The shorter ignition delay exhibited by the gamma lactones is therefore expected. [40] The rate of the low temperature reactions which propagate radical formation increase with alkyl chain length, as a higher number of six or seven membered transition states can form. [41] Apparent also in Fig. 4.5b is that increasing the alkyl chain length in both the gamma and delta lactones shortens the duration of ignition delay. This is an expected result as increasing alkyl chain length has previously been shown to shorten the duration of ignition delay in straight chain alkane single component fuels. [29].

Plotting according to substituent alkyl chain length (Fig. 4.5b) further shows that at lengths of 4 to 6 carbons, the delta lactones exhibit a shorter ignition delay. This is also expected, as the delta lactone ring contains one additional –CH $_2$ group and for equivalent lactones with the same chain lengths the delta lactones constitute a higher calorific value. At a chain length of 4 carbons this difference is most pronounced and this is not surprising given the lactones which contained fewer carbons than gamma octalactone did not combust. γ Ol is the first lactone to

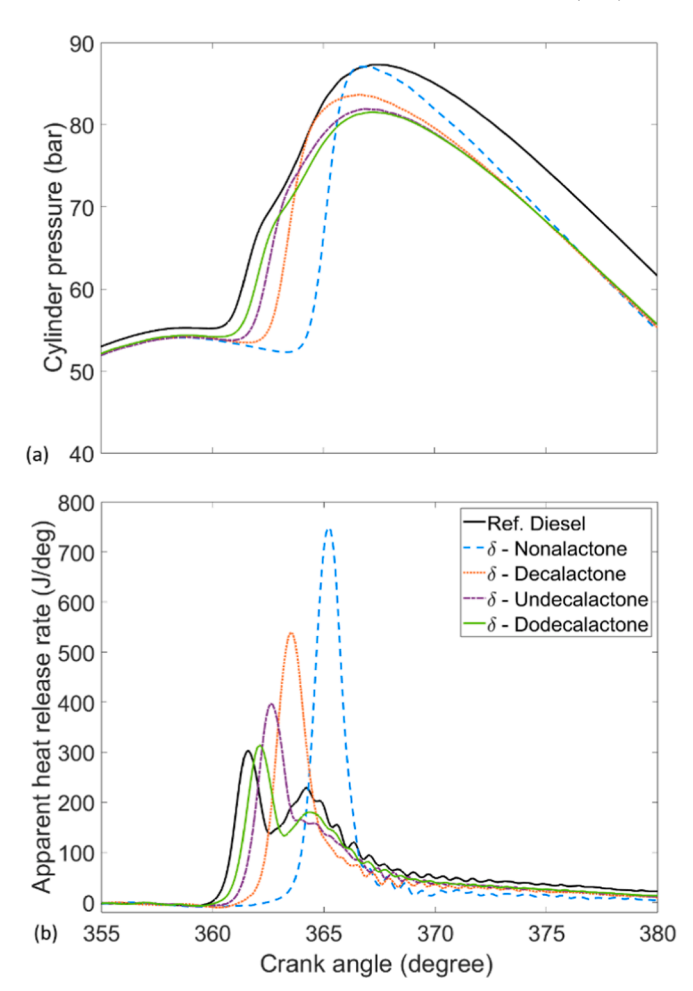


Fig. 4.2. (a) In-cylinder pressures and (b) apparent net heat release rates of the single component delta lactone test fuels and reference fossil diesel.

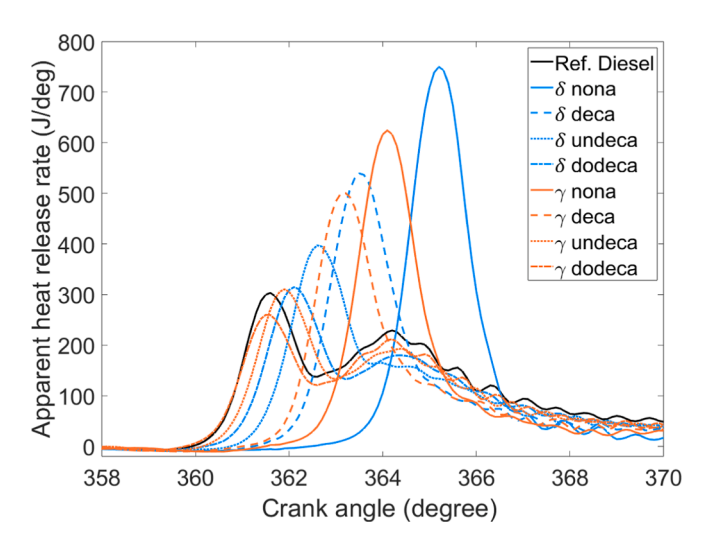


Fig. 4.3. The apparent net heat release rate of the delta and gamma lactone single component test fuels with a total carbon count of C9 to C12 and the reference fossil diesel.

exhibit stable combustion and the delta lactone with an equivalent alkyl chain length would have a lower carbon to oxygen ratio, increasing the likelihood of stable combustion occurring.

In agreement with previous findings from Frost et al. [24], γDdl exhibited a shorter duration of ignition delay than the reference fossil

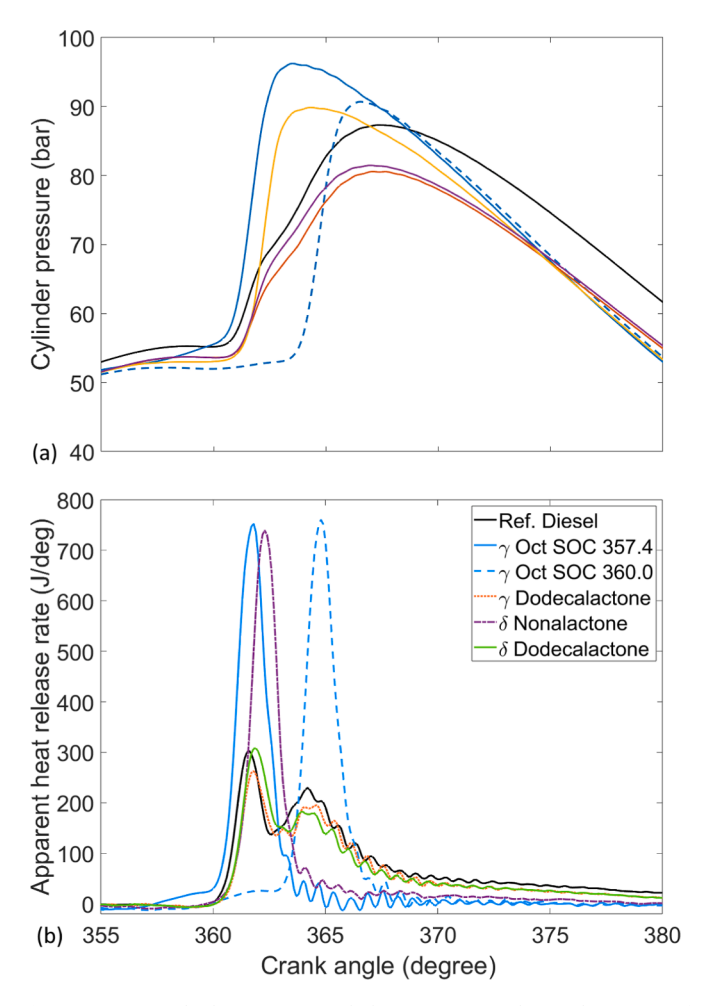


Fig. 4.4. (a) In-cylinder pressure and (b) apparent net heat release rate of gamma octalactone, gamma dodecalactone, delta nonalactone, delta dodecalactone single component test fuels and reference fossil diesel variable injection timing for constant start of combustion at TDC, or for the second stage of γ Ol to occur at TDC.

diesel, despite a significant difference in test facilities and experimental considerations. The D8k used for this work was a heavy-duty engine while that used by Frost et al. a high-speed passenger vehicle one; the

D8k had a combustion chamber volume over 2.5 times larger, was operated at 2/3rd the speed and double the IMEP. Additionally, γDdl was tested as a single component fuel here, but was tested only as a blend with butanol and diesel by Frost et al.

A surprising result shown in Fig. 4.5 is that γUl exhibits a shorter ignition delay than both δUl and δDdl . As shown in Table 3.1, δDdl has a higher carbon count and calorific value, so it could be expected that δDdl would have a shorter ignition delay than γUl .

The shorter ignition delay of γUl than δDdl may imply that the gamma ring structure does uniquely influence the duration of ignition delay in addition to the inherent longer carbon chain length for equivalent carbon numbers. This could be attributed to higher reactivity caused by their configuration. In cyclic organic molecules, the 6 membered ring configuration experiences less ring strain than all other potential organic rings. Ring strain is a property which emerges from repulsive forces of electrons held in atomic bonds. In the simplest organic molecule, methane (CH₄) the angles between C-H bonds are 109.5° and this is the lowest energetic arrangement. If the bonds were forced to have a smaller internal angle, a repulsive force arises between electrons held in the bonds. In a 6 membered ring the bonds forming the structure can arrange such that the internal angles are closest to that of methane compared to all other ring sizes. The increased ring strain experienced by 5-membered rings is attributed to a higher reactivity and heat of combustion. [42,43] The ring strain in lactones however present counter-intuitively to this as the ester functional group has different bonding angles to hydrocarbons. Instead, gamma lactones hold a slightly lower ring strain energy than delta lactones, but how this changes with an alkyl substituent has not been investigated. [44].

Fig. 4.6 shows the IMEP of the gamma lactones, delta lactones and the reference diesel, shown both against the lactone size and substituent alkyl chain length at constant injection duration. γ Ol, γ Ddl, δ Nl and δ Ddl were tested at both the constant injection and constant SOC test conditions. γ Ol experiences two-stage ignition and a second test was performed with the 2nd stage of ignition occurring at TDC with an injection timing of 11.7 CAD BTDC.

For both the gamma and delta lactones the IMEP increases with lactone size, with the trend becoming less apparent as the lactone size increases and the IMEP converges. The error for the reference diesel is 0.09 bar and as shown in Table 3.2 this value is larger than the difference in IMEP exhibited between the undeca and dodeca lactones. Additionally, δNl and δDl both exhibit a higher IMEP than γNl and γDl respectively, whilst the larger lactones δUl and δDdl exhibit a lower IMEP than γUl and γDdl respectively. Prior to the convergence in IMEP exhibited by the lactones at carbon numbers greater than C10, it is clear that the delta

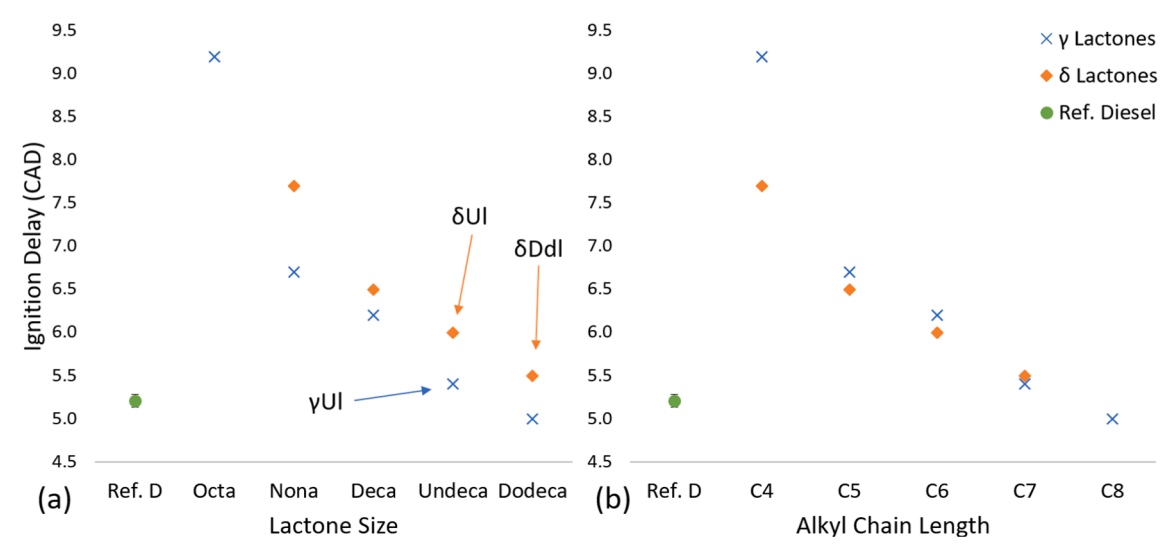


Fig. 4.5. Variation of ignition delay with (a) lactone carbon number and (b) lactone alkyl chain length at constant injection timing.

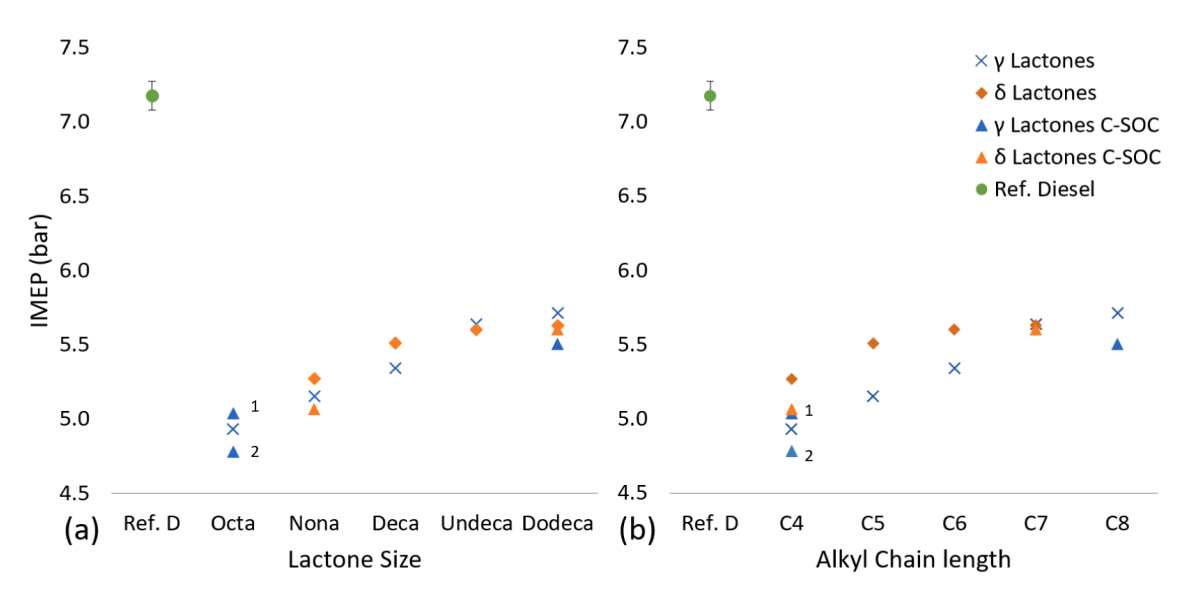


Fig. 4.6. Indicated mean effective pressure (IMEP) of the lactone single component fuels and reference diesel, tested at constant injection timing and duration. Additionally, some data is shown at constant start of combustion at TDC (C-SOC) which required varying of injection timing. Note that data label 1 corresponds to γ Ol 1st ignition at TDC, and 2 γ Ol 2nd ignition at TDC.

isomer exhibits a higher IMEP than the gamma isomer.

The convergence in IMEP exhibited by the lactones at first seems unintuitive, as increasing the carbon size, calorific value and length of straight alkyl chains in the single component fuels all increase the amount of available energy in the chamber during combustion. However, when moving to the larger lactones and the carbon numbers increase, the proportional decrease in lactone oxygen becomes less pronounced. Moving from an octa to nona lactone changes the carbon to oxygen ratio more significantly than going from an undeca to dodeca lactone. Additionally, as shown in Table 3.1, as the lactone size increases in both the delta and gamma lactones, the density decreases and viscosity increases. The combustion tests were undertaken at a constant injection duration with no correction for fuel volume or mass. Under these conditions, a lower fuel density and a higher fuel viscosity would both reduce the mass of fuel entering the chamber each combustion cycle. Kim et al. (2019) investigated how fuel viscosity impacts fuel spray behaviour and found that increasing viscosity will reduce the injected mass of fuel. [45] In the case of the lactone single component fuels, it is feasible that the higher calorific value of the dodecalactones than the undecalactones is offset by lower mass of fuel and therefore energy available during combustion.

Finally, a trend observed at the constant SOC test conditions is the slight reduction in IMEP when γOl 's second-stage ignition occurred at TDC relative to the first stage occurring at TDC. Despite the same amount of energy available, if the first stage of ignition occurs prior to TDC then chemical energy is resisting the compression stroke instead of providing useful work in the expansion stroke. γDdl and δDdl ignited close to TDC under the constant injection timing condition, and the small change in injection timing necessary to ensure ignition at TDC was not sufficient to change the measured IMEP significantly (Fig. 4.6).

Fig. 4.7 shows the peak apparent heat release rate of the gamma lactones, delta lactones and the reference diesel. The trend apparent from both subfigures is that with the exception of γ Ol tested at the constant injection timing condition, increasing lactone size in both the

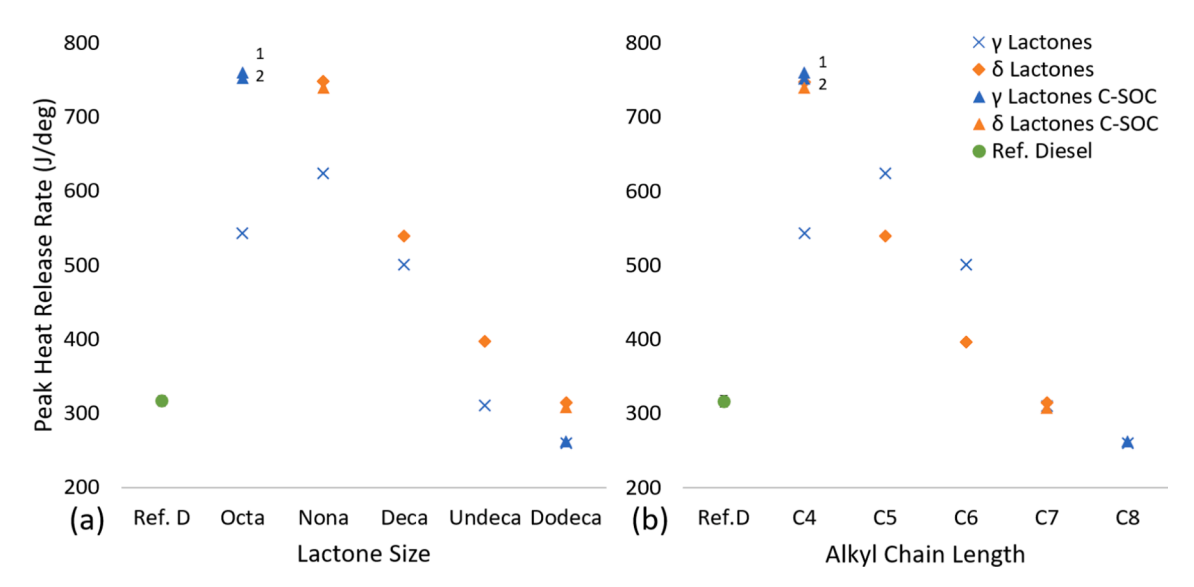


Fig. 4.7. Peak apparent heat release rate of single component gamma and delta lactone test fuels and reference diesel, tested at constant injection timing and duration. Additionally, some data is shown at constant start of combustion at TDC (C-SOC) which required varying of injection timing. Note that data label 1 corresponds to γ Ol 1st ignition at TDC, and 2 γ Ol 2nd ignition at TDC.

gamma and delta lactones decreases the magnitude of APHRR observed. The sensitivity to the injection timing for γ Ol implies that bringing forward the injection timing and bringing ignition closer to TDC is necessary for clarifying how γ Ol should behave in trend with larger lactones. It is shown in Fig. 4.7a that for each lactone size the gamma lactone exhibits a lower APHRR than the delta lactone, in agreement with the observed longer ignition delay of the equivalent carbon number delta lactones (Fig. 4.5a). As the duration of ignition delay directly impacts the APHRR, as longer durations allow for greater air–fuel mixing to occur prior to combustion, thus increasing the extent of the premixed burn fraction. [46,47].

It is interesting to note however that the APHRR exhibited by γOl at constant injection timing does not correlate with the observed relationship between APHRR and the duration of ignition delay. As shown in Fig. 4.1, γOl exhibited two-stage ignition, with two distinct periods of change in the rate of heat release. It has previously been suggested that single component fuels exhibiting two-stage ignition strongly facilitate chain propagation over chain branching reactions during the low temperature period of combustion. [48] Chain propagation reactions maintain a constant number of radicals within the system, whereas chain branching increase the number of radicals. The cool combustion time period between the first and second ignition delay will partially oxidise the fuel. [49] Partial fuel oxidation would reduce the potential for energy release during the second ignition stage, a possible cause for the observed peak heat release rate of γOl being lower than γNl despite a longer ignition delay.

Bringing forward the injection timing of γOl so that either the 1st or 2nd stage of ignition occurs at TDC significantly increases the APHRR, at constant SOC timing γOl displays the longest duration of ignition delay and highest peak heat release rate. The 1st or 2nd stage of ignition occurring at TDC does not significantly change the APHRR any further, additionally changing the injection timing of δNl also does not significantly impact the APHRR. This implies that the low APHRR observed during combustion of γOl at constant injection timing could instead be caused by the geometry of the combustion chamber during this time and not the chemical properties of the fuel. At the time of autoignition, the piston will have moved away from TDC, exposing more of the cylinder walls, providing more surface area for the transfer of heat away from the air fuel mixture. γOl auto-ignites 3.9 CAD after TDC during which the incylinder pressure and temperature have both decreased, leading to less efficient combustion.

Fig. 4.8 shows the calculated duration of combustion of the gamma lactones, delta lactones and the reference diesel, defined as the period

between the start of combustion and the first appearance of a negative heat release rate following the occurrence of APHRR. The trend apparent is that increasing lactone size increases the duration of combustion. Previously shown in Fig. 4.1 and Fig. 4.2 were the heat release plots during combustion of the lactone single component fuels. As previously mentioned, increasing lactone size reduced the duration of ignition delay, so less time was available for air fuel mixing prior to autoignition. Increasing lactone size therefore leads to a smaller premixed burn phase and increase in the less rapid mixing-controlled phase of combustion. Further, apparent is lack of difference in combustion duration between the delta and gamma deca, undeca and dodecalactones, indicating that gamma / delta ring size isomerism does not impact duration of combustion once a total carbon number has been surpassed. For lactones with the same alkyl chain length, the delta lactones have a slightly longer duration, clearly indicating that the total carbon to oxygen ratio has a bigger impact on duration of combustion than gamma / delta lactone isomerism as for equivalent chain lengths the delta lactones larger ring size will always result in a higher carbon to oxygen ratio.

A further observation is that bringing forward the injection timing reduces the duration of combustion of δNl and γOl with both injection timings.

4.4. Exhaust emissions

Fig. 4.9 shows the measured NO_x emissions during combustion of the delta lactones, gamma lactones and the reference diesel at constant injection timing conditions; a subset of the fuels were further tested at constant ignition timings, requiring injection timing to be varied.

Immediately apparent is the significant increase in NO_x emissions resultant from γOl and δNl relative to both diesel and the other lactones tested. Given the low global equivalence ratio and lean combustion environment of a diesel engine, it could be expected that γOl and δNl would instead exhibit lower NOx emissions than the remaining lactones which have a more pronounced diffusion controlled combustion phase (Fig. 4.3), during which the majority of NOx is typically produced as global in-cylinder temperatures rise. [47] The observed higher NOx emissions displayed by γOl and δNl can instead be attributed to higher peak combustion temperatures associated with the long ignition delays exhibited by each (Fig. 4.5). Longer ignition delay allows for greater air fuel mixing prior to autoignition, leading to combustion dominated by the premixed burn fraction and a short duration of combustion. [50] The extent of heat release during this phase (Fig. 4.7) and the resulting

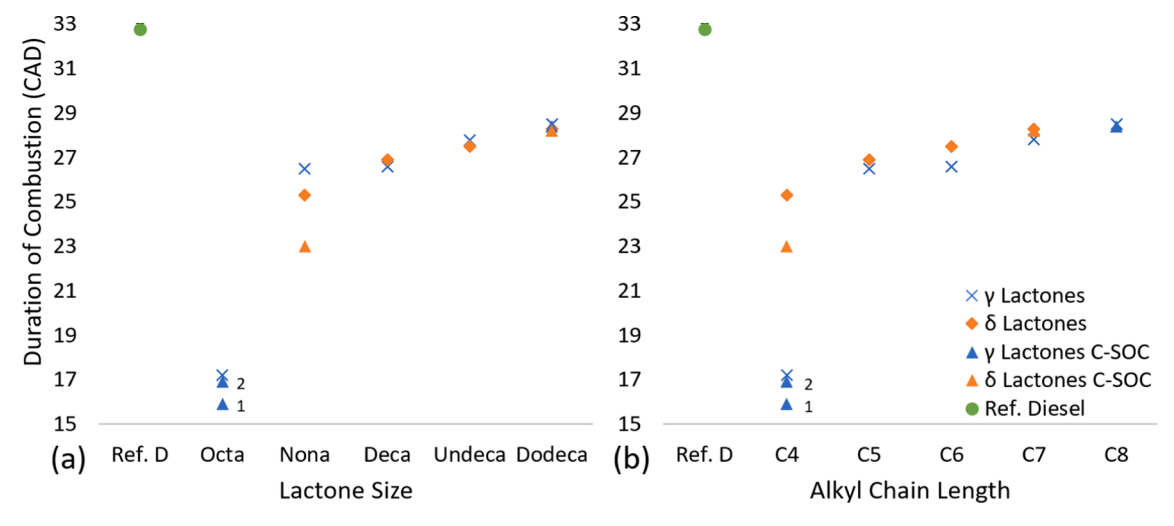


Fig. 4.8. Calculated duration of combustion of single component gamma and delta lactone test fuels and reference diesel, tested at constant injection timing and duration. Additionally, some data is shown at constant start of combustion at TDC (C-SOC) which required varying of injection timing. Note that data label 1 corresponds to γ Ol 1st ignition at TDC, and 2 γ Ol 2nd ignition at TDC.

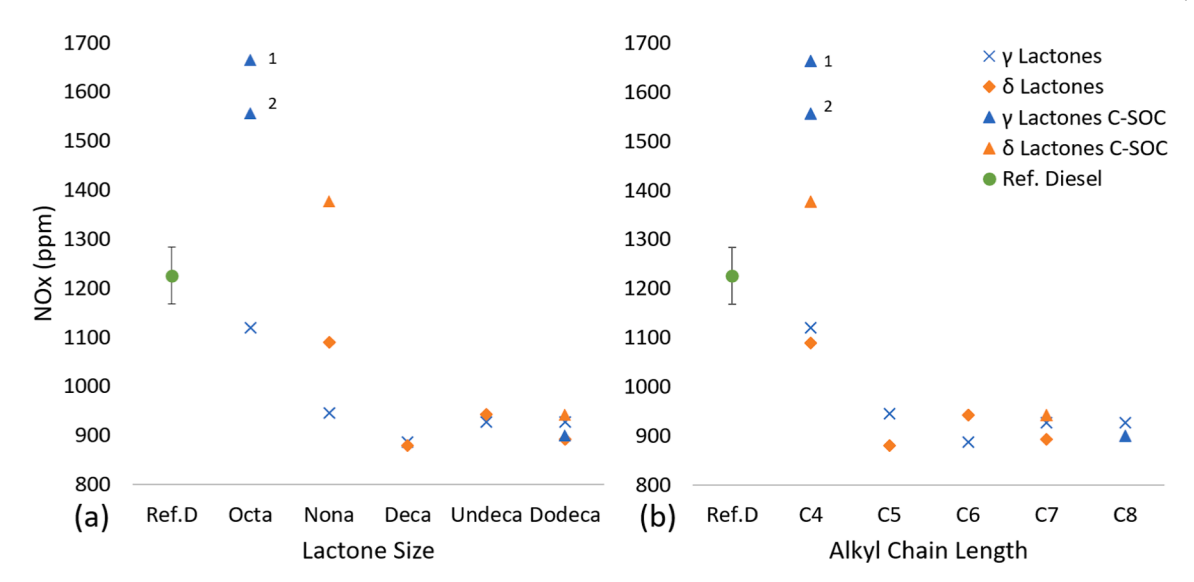


Fig. 4.9. Exhaust gas NO_x emissions of the delta lactone and gamma lactone single component fuels and reference diesel vs lactone structure, tested at constant injection timing and duration. Additionally, some data is shown at constant start of combustion at TDC (C-SOC) which required varying of injection timing. Note that data label 1 corresponds to γ Ol 1st ignition at TDC, and 2 γ Ol 2nd ignition at TDC.

higher peak in-cylinder temperatures lead to exponential rise in NOx formation rate and is more significant than the duration of mixing controlled combustion in determining exhaust levels of NOx at the conditions tested (Section 3).

NOx production is highly time dependent, as the thermochemistry kinetics will 'freeze' during the expansion stroke as the in-cylinder temperature and pressure both decrease during gas expansion. [51–55] Changing the injection timing to facilitate combustion of γ Ol at TDC causes an intense, short premixed flame to dominate the combustion process which quickly consumes all the fuel as shown by the short duration of combustion (Fig. 4.8). Reaching a higher temperature and completing combustion 6-7 CAD faster than γ Dl and γ Nl allows more time for the hot gaseous combustion products to remain at high temperature prior to freezing of NOx kinetics. [55].

Apparent is the lower NO_x emissions detected during combustion of the single component test fuels compared to the reference diesel at the constant injection timing test condition. NOx production also relies on the residence time of gases at high temperature and pressure, close to

stoichiometric ratios, with high production typically occurring during the mixing-controlled combustion phase for fossil diesel. Thermal production of NO_x at high rates requires temperatures above about 1600 K and while each of the lactone test fuels displayed average temperatures of 1700–1800 K (previously shown in Table 3.2), the reference diesel exhibits a significantly higher temperature of 1900 K, higher IMEP and longer duration of combustion, so therefore the lower NOx emissions of the lactones are to be expected as the hot gaseous combustion products are held above 1600 K for a longer period of time. [56].

Fig. 4.10 shows the unburnt hydrocarbon emissions of the two groups of lactone single component fuels and the reference diesel at constant injection conditions and subset of the fuels tested at constant SOC at TDC (varied ignition timings).

Immediately apparent is the significantly high THC value of γOl which can be attributed to the observed long ignition delay and resultant premixed burn faction dominating combustion. A long duration of ignition delay allows for greater air fuel mixing, creating areas of over-diluted fuel spray within the chamber which are too lean to auto-ignite

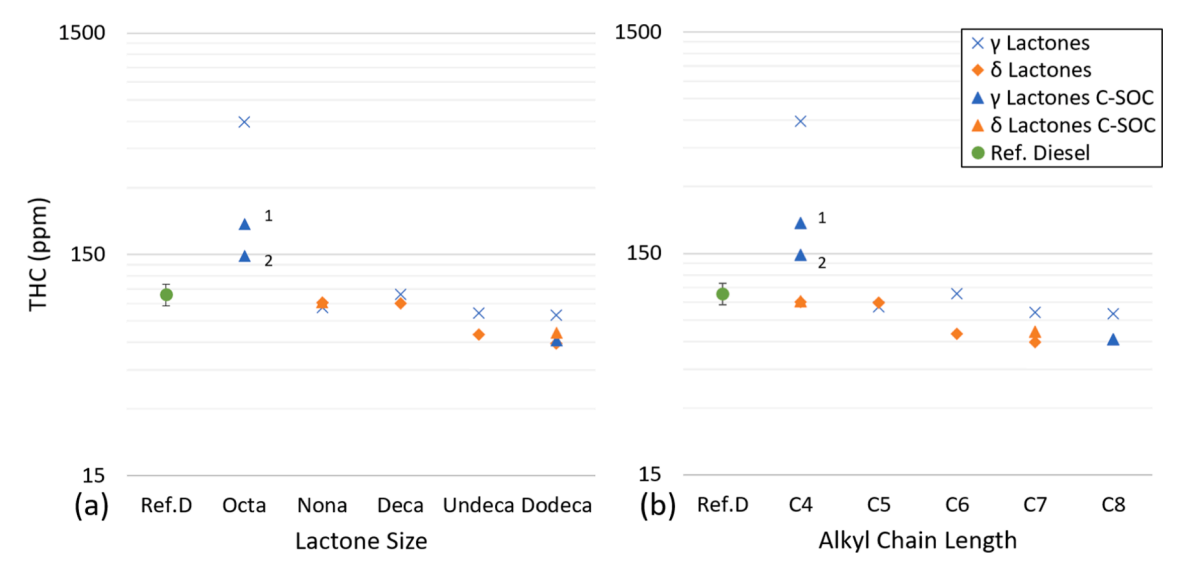


Fig. 4.10. Exhaust gas unburnt hydrocarbon emissions of the gamma lactones, delta lactones and reference diesel, vs lactone size & substituent alkyl chain length, tested at constant injection timing and duration. Additionally, some data is shown at constant start of combustion at TDC (C-SOC) which required varying of injection timing. Note that data label 1 corresponds to γ Ol 1st ignition at TDC, and 2 γ Ol 2nd ignition at TDC. (Note logarithmic vertical scales).

or support a self-propagating flame, increasing the amount of un-reacted fuel. Bringing forward the injection timing such that the 1st or 2nd stage of ignition occurs at TDC significantly reduced the THC measured during combustion. As previously mentioned, the significantly delayed SOC of γ Ol under the constant injection testing condition resulted in combustion occurring at a lower pressure and temperature, lowering the overall efficiency of the combustion process.

Further apparent is the lower levels of THC emissions resultant from the delta deca, undeca and dodeca lactones than the gamma lactones. This is unexpected as THC arising from over lean mixtures resultant from long durations of ignition delay are assumed to be the most important contributor to THC formation, but for each equivalent lactone the delta isomer exhibits a longer ignition delay (Fig. 4.5). [50] The delta lactones all exhibit a higher viscosity than the equivalent gamma isomers and unburnt hydrocarbons typically result from air fuel mixture too lean or too rich to sustain combustion. The slightly lower viscosity of the gamma lactones versus their equivalent delta isomer may have caused some fuel droplets to penetrate and spread further into the chamber prior to autoignition and become too lean to ignite. [57] It is also interesting to note that the relatively high viscosities of the larger lactones (Table 3.1) does not appear to worsen combustion or result in higher THC emissions, as might be expected from higher viscosities limiting air fuel mixing, resulting in incomplete combustion.

Fig. 4.11 shows the CO emissions during combustion of the delta lactones, gamma lactones and reference diesel at constant injection conditions and subset of the fuels tested at constant SOC (varied injection timings).

Strikingly apparent is the significantly higher emissions resulting from combustion of γ Ol at each injection timing and δ Nl. The measured CO from both γ Ol and δ Nl significantly reduces as the injection timing is brought forwards. CO is a product from incomplete combustion and the significant duration of ignition delay exhibited by γ Ol and δ Nl leads to autoignition and premixed combustion occurring further into the expansion stroke than the remaining lactones. Bringing forward the time of injection timing ensures that autoignition occurs closer to TDC, which is the point of highest pressure and heat in the combustion chamber during the four-stroke cycle. Additionally, the long ignition delays of γ Ol and δ Nl (Fig. 4.5) resulted in a large premixed burn fraction, during which there was more time for fuel at the leading edge of the spray to diffuse away from the flame fronts formed during autoignition and thus experienced incomplete combustion. As the carbon number increased and ignition delay decreased, the combustion profile of the lactones was

more dominated by a mixing-controlled flame (Fig. 4.3), resulting in more complete combustion.

Further apparent is the reduction in CO emissions as lactone size increases and the higher CO emissions detected during combustion of the delta lactones over their equivalent gamma isomer. This trend matches the trend observed in ignition delay and the premixed burn fraction of combustion. As mentioned above, longer duration of ignition delay allows for greater air fuel mixing and the formation of over-lean mixture in the chamber which may not auto ignite or fail to sustain a self-propagating flame, resulting in incomplete combustion. [58] The previous observed trend in ignition delay (Fig. 4.5) was that of the alkyl chain length having greatest influence on the duration of delay, whilst the total lactone size had greater influence on the CO results which also reflect the differences in boiling point between the lactones (Table 3.1).

Fig. 4.12 shows the particle number size distribution of γ Ol, γ Ddl, δ Nl, δ Ddl and the reference diesel tested at the constant SOC at TDC test condition.

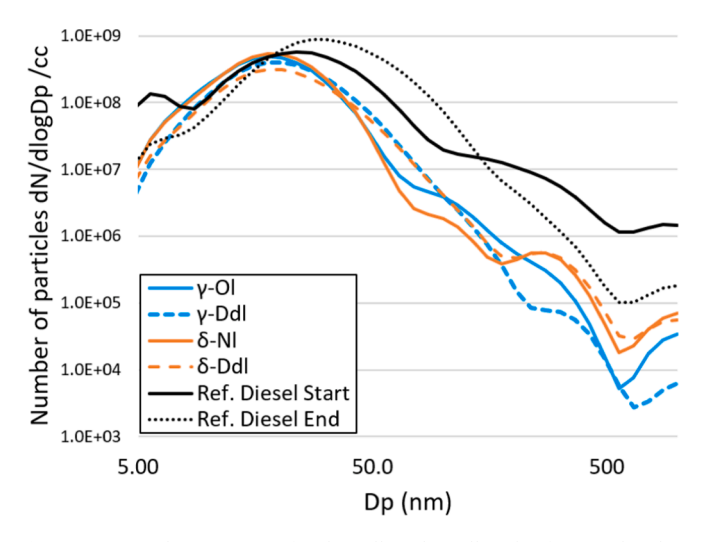


Fig. 4.12. Particle emissions of γOl , γDdl , δNl , δDdl and reference diesel at constant start of combustion at TDC. Ref. Diesel start is the first test performed before the lactone tests and Ref. Diesel end is the final test performed after the set of lactones were tested. Both are included to show the influence a full day of combustion tests has on the reference diesel's particulate formation.

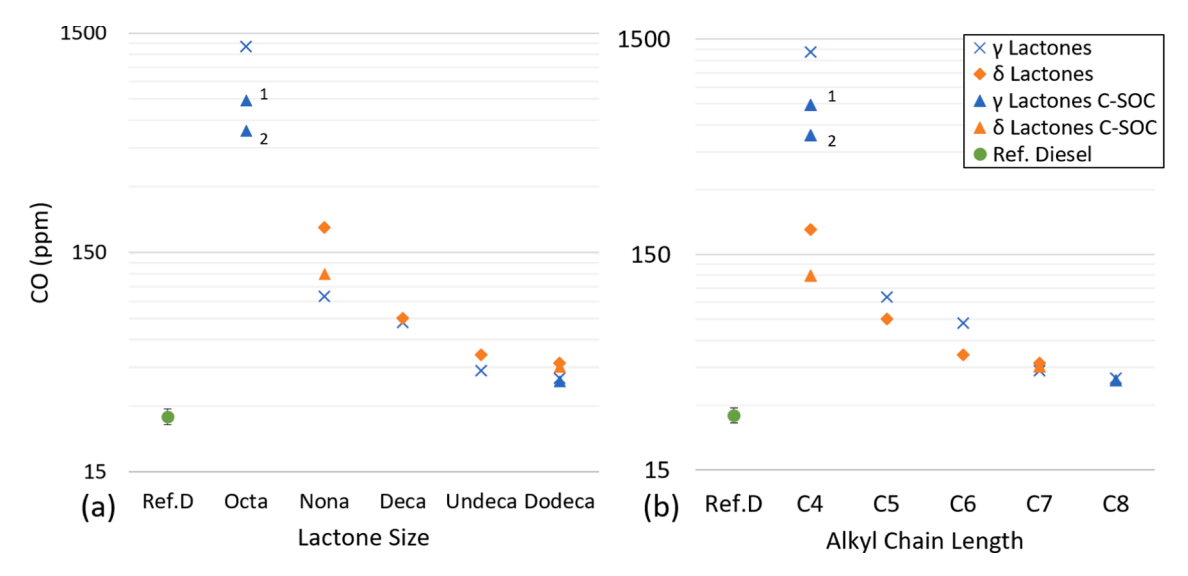


Fig. 4.11. Exhaust gas CO emissions of the delta lactones, gamma lactones and reference diesel vs lactone size, tested at constant injection timing and duration. Additionally, some data is shown at constant start of combustion at TDC (C-SOC) which required varying of injection timing. Note that data label 1 corresponds to γ Ol 1st ignition at TDC, and 2 γ Ol 2nd ignition at TDC. (Note logarithmic vertical scales).

Apparent is that all fuels showed a similar peak in the number of particles in the nucleation size range (Dp ≤ 50 nm). The gamma lactones then emit very similar or a lower number of accumulation mode particles (50 \leq Dp \leq 500 nm) than the delta lactones. Compared to the reference fossil diesel all the lactones emit fewer particles at particle sizes larger than 15 nm, which differs from the previous investigation by Frost et al. which found that lactone and diesel fuel blends emitted a higher number of nucleation mode particulates than fossil diesel.

Fig. 4.13a shows the total particulate count and Fig. 4.13b shows the total particulate mass measured during combustion of γ Ol, γ Ddl, δ Nl, δ Ddl and reference fossil diesel, at constant start of combustion.

Apparent is the reduction in total particulate count as lactone size increases. γDdl exhibits a lower total count than δDdl , implying the gamma lactones typically emit fewer particles than their delta lactone counterparts, but particulate measurements from further lactone pairs would be required to confirm this. From the data available, it appears ignition delay is the determinant factor on total particulate count, as the dodecalactones which exhibited short durations of ignition delay emitted a lower particulate count. Despite being an oxygenated species, γOl emits a relatively higher total particular mass than the other lactones, attributable to its longer duration of ignition delay and short duration of combustion, leaving little time for continued oxidation of any particulate species formed prior to opening of the exhaust valves.

Of final note, there is a slight increase in total mass emitted by the delta lactones as lactone size increases, implying that despite the reduction in particulate count, δDdl does not see a reduction in particulate precursors during combustion.

5. Conclusions

In addition to all of the scientific detail from the results, this work is the first to discuss heavy-duty compression ignition engine tests designed to investigate the potential differences in combustion caused by delta / gamma lactone isomerism and effects caused by increasing the length of a substituent alkyl chain.

- A series of gamma and delta lactones with an alkyl chain substituent were tested as single component test fuels and were found to ignite and undergo stable combustion in a heavy-duty diesel engine.
- Increasing the length of the alkyl substituent chain on both lactone isomers (increasing their total carbon count) was found to reduce the duration of ignition delay, increase the duration of combustion, and decrease the measured emissions of nitrogen oxides, unburnt hydrocarbons, carbon monoxide and particulates.

- Gamma Undecalactone exhibits a shorter ignition delay than all the gamma lactones with a smaller carbon count, as would be expected, but it further exhibits a shorter ignition delay than delta lactones with a higher carbon count indicating that gamma lactones may directly shorten the duration of ignition delay.
- Gamma lactones with an increasing substituent alkyl chain with a total carbon count of 8 to 12 exhibit shorter ignition delays than their delta isomers, likely resulting from a higher reactivity derived from their ring strain.

The slight reduction in unburnt hydrocarbons and increase in carbon monoxide in delta lactones could be attributed to their slightly longer duration of ignition delay compared to the gamma lactones.

Further studies could be performed to investigate the particulate emissions from the full set of lactones as time constraints prevented a full investigation.

In this study of lactone isomerism, it was observed that gammaundecalactone exhibited a lower duration of ignition delay than all of the tested delta lactones. The observed trend of shorter ignition delays with a longer alkyl chain in both lactone isomers was clearly becoming less pronounced as the lactones became larger, and so it would be interesting in future work to see if the ignition delay of gammaundecalactone is shorter than delta-tridecalactone. It would also be of interest to test if after a certain carbon chain length, the ignition delay of both isomers no longer reduces and whether the two isomers converge or the gamma lactones will always exhibit a shorter duration of ignition delay than the delta lactones. It should be noted that whilst the lactones tested in this work can be easily sourced from biomass, larger lactones become increasingly rare and unlikely to be sourced in any meaningful quantity, so the suggestions here for further work would strictly be for academic interest.

CRediT authorship contribution statement

Timothy Deehan: Writing – review & editing, Writing – original draft, Visualization, Validation, Software, Resources, Methodology, Investigation, Formal analysis, Data curation, Conceptualization. Paul Hellier: Writing – original draft, Supervision, Resources, Project administration, Funding acquisition, Conceptualization. Nicos Ladommatos: Writing – original draft, Supervision, Resources, Project administration, Funding acquisition, Conceptualization.

Declaration of competing interest

The authors declare that they have no known competing financial

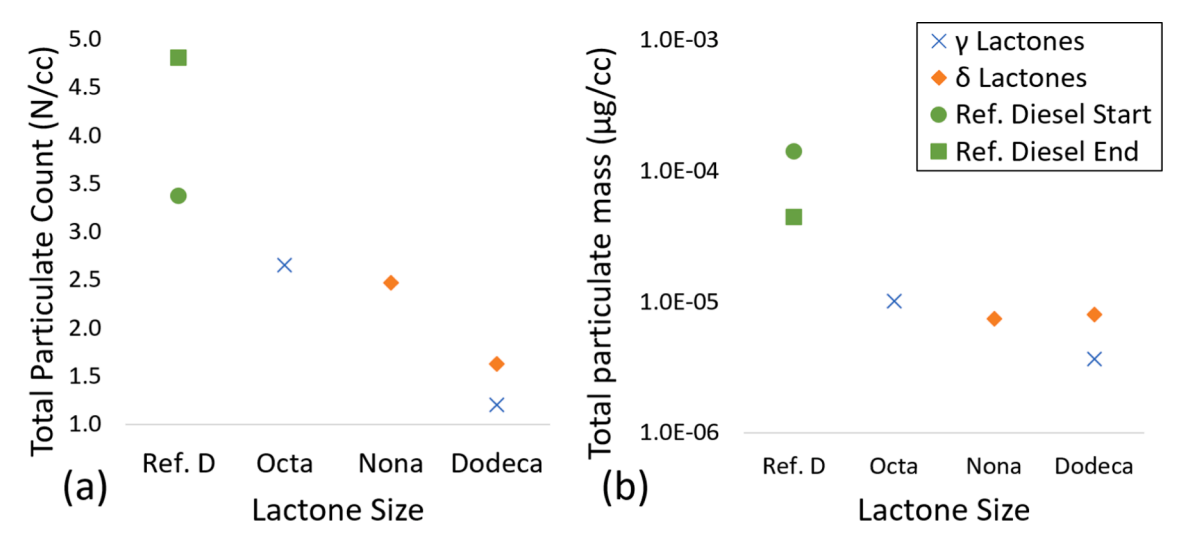


Fig. 4.13. Total particulate count (a) and total particulate mass (b) emitted from γOl, γDdl, δDdl and reference fossil diesel at constant SOC at TDC.

interests or personal relationships that could have appeared to influence the work reported in this paper.

Data availability

Data will be made available on request.

References

- [1] Westerhold, T., Marwan, N., Drury, A. J., Liebrand, D., Agnini, C., Anagnostou, E., et al. An astronomically dated record of Earth's climate and its predictability over the last 66 million years. Science (80-.). 369, 1383–1388 (2020).
- [2] Moss RH, Edmonds JA, Hibbard KA, Manning MR, Rose SK, Van Vuuren DP, et al. The next generation of scenarios for climate change research and assessment. *Nature* 2010;463:747–56.
- [3] Shaftel H, Callery S, Jackson R, Biley D. Evidence | Facts Climate Change: Vital Signs of the Planet. Earth Science Communications Team at NASA's Jet Propulsion Laboratory, 2023.
- [4] Retrieved Oct 2019;11:2021. from, https://ec.europa.eu/info/strategy/priorities-2019-2024/european-green-deal_en.
- [5] European Commission. European Commission-Press release European Green Deal: EU agrees stronger legislation to accelerate the rollout of renewable energy. (2023)
- [6] Francis AC, Robert MG. Organic Chemistry. McGraw-Hill; 2011.
- [7] Su J, Shen F, Qiu M, Qi X, Farmer TJ, Clark JH. High-yield production of levulinic acid from pretreated cow dung in dilute acid aqueous solution. *Molecules* 2017;22.
- [8] Coricello A, Adams JD, Lien EJ, Nguyen C, Perri F, Williams TJ, et al. A Walk in Nature: Sesquiterpene Lactones as Multi-Target Agents Involved in Inflammatory Pathways. Curr Med Chem 2018;27:1501–14.
- [9] Schrader J, Etschmann MMW, Sell D, Hilmer J-M, Rabenhorst J. Applied biocatalysis for the synthesis of natural flavour compounds. *Biotechnol Lett* 2004; 26:463–72
- [10] da Silva Souza IH, Nogueira JP, Chaves RV, Sandes RDD, Leite Neta MTS, Narain N. Microbial lactones: A systematic bibliometric review of γ-lactone production by biotechnological processes and technological prospection with focus on γ-dodecalactone. Biocatal Agric Biotechnol 2024;60:103318.
- [11] Syed N, Singh S, Chaturvedi S, Nannaware AD, Khare SK, Rout PK. Production of lactones for flavoring and pharmacological purposes from unsaturated lipids: an industrial perspective. Crit Rev Food Sci Nutr 2023;63:10047–78.
- [12] Chaffey DR, Bere T, Davies TE, Apperley DC, Taylor SH, Graham AE. Conversion of levulinic acid to levulinate ester biofuels by heterogeneous catalysts in the presence of acetals and ketals. Appl Catal B Environ 2021;293:120219.
- [13] Boot, M. D. Use of a perfume composition as a fuel for internal combustion engines. (Patent No. WO2013032321). World Intellectual Property Organization (2013).
- [14] Kourist R, Hilterhaus L. Microbial Lactone Synthesis Based on Renewable Resources 2015;275–301. https://doi.org/10.1007/978-3-662-45209-7 10.
- [15] Kaori Nakano A, Botelho Lourenco C, Calvet F, Carrasco C. A method for improving the performance of a fragrance or a fragrance mixture 2020;95–98.
- [16] Liang X, Duan Y, Fan Y, Huang Z, Han D. Influences of C5 esters addition on antiknock and auto-ignition tendency of a gasoline surrogate fuel. *Int J Engine Res* 2021. https://doi.org/10.1177/14680874211030898.
- [17] Isikgor FH, Becer CR. Lignocellulosic biomass: a sustainable platform for the production of bio-based chemicals and polymers. *Polym Chem* 2015;6:4497–559.
- [18] Talibi M, Hellier P, Ladommatos N. Investigating the Combustion and Emissions Characteristics of Biomass-Derived Platform Fuels as Gasoline Extenders in a Single Cylinder Spark-Ignition Engine. SAE Tech Pap 2017–01–2325 (2017). https://doi. org/10.4271/2017-01-2325.
- [19] Chidambaram K, Ashok B, Vignesh R, Deepak C, Ramesh R, Narendhra TMV, et al. Critical analysis on the implementation barriers and consumer perception toward future electric mobility. Proc Inst Mech Eng Part D J Automob Eng 2022. https://doi. org/10.1177/09544070221080349.
- [20] Fleming KL, Brown AL, Fulton L, Miller M. Electrification of Medium- and Heavy-Duty Ground Transportation: Status Report. Curr Sustain Energy Reports 2021;8: 180-8
- [21] Ayodele OO, Dawodu FA, Yan D, Lu X, Xin J, Zhang S. Hydrodeoxygenation of angelica lactone dimers and trimers over silica-alumina supported nickel catalyst. *Renew Energy* 2016;86:943–8.
- [22] Yan K, Lafleur T, Wu X, Chai J, Wu G, Xie X. Cascade upgrading of γ -valerolactone to biofuels. *Chem Commun* 2015;51:6984–7.
- [23] Bereczky Á, Lukács K, Farkas M, Dóbé S. Effect of γ-Valerolactone Blending on Engine Performance, Combustion Characteristics and Exhaust Emissions in a Diesel Engine. Nat Resour 2014:05:177–91.
- [24] Frost J, Hellier P, Ladommatos N. Bio-derived lactones Combustion and exhaust emissions of a new class of renewable fuels. Energy Convers Manag 2023;283.
- [25] Ratcliff, M. A., Mccormick, R. L. & Taylor, J. D. Compendium of Experimental Cetane Numbers Compendium of Experimental Cetane Numbers. (2017).
- [26] Gil S, Parra M, Rodriguez P, Segura J. Recent Developments in y-Lactone Synthesis. Mini Rev Org Chem 2009;6:345–58.
- [27] Deehan T, Hellier P, Ladommatos N. The influence of Michael acceptors on the structural reactivity of renewable fuels. Sustain Energy Fuels 2024;8.

- [28] Heywood JB. Heat-Release-Rate analysis. Internal Combustion Engine Fundamentals. 2e 858–860. (McGraw-Hill Education; 2018.
- [29] Hellier P, Ladommatos N, Allan R, Payne M, Rogerson J. The impact of saturated and unsaturated fuel molecules on diesel combustion and exhaust emissions. SAE Tech Pap 2011;5:106–22.
- [30] Schönborn A, Ladommatos N, Williams J, Allan R, Rogerson J. Effects on diesel combustion of the molecular structure of potential synthetic bio-fuel molecules. SAE Tech Pap 2007-Septe, (2007).
- [31] Wang S, Zhao Y, Lin H, Chen J, Zhu L, Luo Z. Conversion of C5 carbohydrates into furfural catalyzed by a Lewis acidic ionic liquid in renewable γ-valerolactone. Green Chem 2017;19:3869–79.
- [32] gamma-hexalactone, 695-06-7. http://www.thegoodscentscompany.com/data/rw1006382.html.
- [33] Jensen, T., John, B. Y., Birkinshaw, H. & Raistrick, H. Cccvii . Studies in the Biochemistry of Micro-Organisms . of Terrestric Acid (Ethylcarolic Acid), a Metabolic Product of Penicillium. 2194–2200 (1936).
- [34] UCHIYAMA, H. [US], WOO, R. A. [US], DUVAL, D. L. [US] & REECE, S. [US]. Compositions comprising cyclodextrin. 14 (2005).
- [35] Api AM, Belsito D, Botelho D, Bruze M, Burton GA, Buschmann J, et al. RIFM fragrance ingredient safety assessment, 4'-methylacetophenone, CAS Registry Number 122-00-9. Food Chem Toxicol 2018;122:S75–83.
- [36] Api AM, Belsito D, Botelho D, Bruze M, Burton GA, Buschmann J, et al. RIFM fragrance ingredient safety assessment, δ-dodecalactone, CAS Registry Number 713-95-1. Food Chem Toxicol 2021;153.
- [37] Tanaka S, Ayala F, Keck JC. A reduced chemical kinetic model for HCCI combustion of primary reference fuels in a rapid compression machine. *Combust Flame* 2003;133:467–81.
- [38] Hellier P, Ladommatos N, Allan R, Rogerson J. Combustion and emissions characteristics of toluene/n-heptane and 1-octene/n-octane binary mixtures in a direct injection compression ignition engine. *Combust Flame* 2013;160:2141–58.
- [39] Perrin CL. In: Physical Organic Chemistry. (Academic Press; 2003. https://doi.org/ 10.1016/B0-12-227410-5/00576-7.
- [40] Hellier P, Talibi M, Eveleigh A, Ladommatos N. An overview of the effects of fuel molecular structure on the combustion and emissions characteristics of compression ignition engines. Proc Inst Mech Eng Part D J Automob Eng 2017; 095440701668745. https://doi.org/10.1177/0954407016687453.
- [41] Zhang Y, Yang Y, Boehman AL. Premixed ignition behavior of C9 fatty acid esters: A motored engine study. Combust Flame 2009;156:1202–13.
- [42] Wiberg KB. The Concept of Strain in Organic Chemistry. Angew Chemie Int Ed English 1986;25:312–22.
- [43] Wade LG. Organic chemistry. (Pearson Prentice Hall; 2006.
- [44] Brown JM, Conn AD, Pilcher G, Leitão MLP, Meng-Yan Y. On the strain energy of 5ring and 6-ring lactones. J Chem Soc Chem Commun 1989;1817–1819. https://doi. org/10.1039/C39890001817.
- [45] Kim J, Lee J, Kim K. Numerical study on the effects of fuel viscosity and density on the injection rate performance of a solenoid diesel injector based on AMESim. Fuel 2019:256.
- [46] Thakkar K, Kachhwaha SS, Kodgire P, Srinivasan S. Combustion investigation of ternary blend mixture of biodiesel/n-butanol/diesel: CI engine performance and emission control. Renew Sustain Energy Rev 2021;137:110468.
- [47] Talibi M, Hellier P, Ladommatos N. Impact of increasing methyl branches in aromatic hydrocarbons on diesel engine combustion and emissions. *Fuel* 2018;216: 579–88.
- [48] Kelly-Zion PL, Dec JE. A computational study of the effect of fuel type on ignition time in homogeneous charge compression ignition engines. *Proc Combust Inst* 2000; 28:1187–94.
- [49] Yamada H, Suzaki K, Tezaki A, Goto Y. Transition from cool flame to thermal flame in compression ignition process 2008;154:248–58.
- [50] Heywood, J. B. Internal combustion engine fundamentals. Choice Reviews Online vol. 1 (McGraw-Hill Education, 2018).
- [51] Hoekman SK, Robbins C. Review of the effects of biodiesel on NOx emissions. Fuel Process Technol 2012;96:237–49.
- [52] Heywood JB. NITROGEN OXIDES. Internal Combustion Engine Fundamentals. 2e 978–1005. (McGraw-Hill Education; 2018.
- [53] B., z. y.. The Oxidation of Nitrogen in Combustion and Explosions. J Acta Physicochim 1946;21:577.
- [54] Masum, B. M., Masjuki, H. H., Kalam, M. A., Rizwanul Fattah, I. M., M Palash, S. & Abedin, M. J. Effect of ethanol-gasoline blend on NOx emission in SI engine. *Renew. Sustain. Energy Rev.* 24, 209–222 (2013).
- [55] Nada Y, Komatsubara Y, Pham T, Yoshii F, Kidoguchi Y. Evaluation of NOx Production Rate in Diesel Combustion Based on Measurement of Time Histories of NOx Concentrations and Flame Temperature. SAE Int J Engines 2014;8:303–13.
- [56] Mueller CJ, Boehman AL, Martin GC. An Experimental Investigation of the Origin of Increased NO $_{\rm X}$ Emissions When Fueling a Heavy-Duty Compression-Ignition Engine with Soy Biodiesel. SAE Int J Fuels Lubr 2009;2:2009–01–1792.
- [57] Chang CT, Farrell PV. A study on the effects of fuel viscosity and nozzle geometry on high injection pressure diesel spray characteristics. SAE Tech Pap 1997;106: 558–67.
- [58] Heywood JB. CARBON MONOXIDE. Internal Combustion Engine Fundamentals. 2e 1005–1010. (McGraw-Hill Education; 2018.